

Neutron-dominant quadrupole collective motion in ^{16}C

H. J. Ong,^{1,*} N. Imai,² N. Aoi,² H. Sakurai,¹ Zs. Dombrádi,³ A. Saito,⁴ Z. Elekes,^{2,3} H. Baba,⁴ K. Demichi,⁵ Z. S. Fülöp,³ J. Gibelin,^{5,6} T. Gomi,² H. Hasegawa,⁵ M. Ishihara,² H. Iwasaki,¹ S. Kanno,⁵ S. Kawai,⁵ T. Kubo,² K. Kurita,⁵ Y. U. Matsuyama,⁵ S. Michimasa,² T. Minemura,² T. Motobayashi,² M. Notani,^{4,†} S. Ota,⁷ H. K. Sakai,⁵ S. Shimoura,⁴ E. Takeshita,⁵ S. Takeuchi,² M. Tamaki,⁴ Y. Togano,⁵ K. Yamada,² Y. Yanagisawa,² and K. Yoneda²

¹*Department of Physics, University of Tokyo, 7-3-1 Hongo, Bunkyo, Tokyo 113-0033, Japan*

²*RIKEN, 2-1 Hirosawa, Wako, Saitama 351-0198, Japan*

³*ATOMKI, H-4001, Debrecen, P.O. Box 51, Hungary*

⁴*CNS, University of Tokyo, RIKEN Campus, 2-1 Hirosawa, Wako, Saitama 351-0198, Japan*

⁵*Department of Physics, Rikkyo University, 3-34-1 Nishi-Ikebukuro, Toshima, Tokyo 171-8501, Japan*

⁶*Institut de Physique Nucléaire, F-91406 Orsay Cedex, France*

⁷*Department of Physics, University of Kyoto, Kitashirakawa, Kyoto 606-8502, Japan*

(Received 1 December 2004; published 27 February 2006)

Inelastic proton scattering to the 2_1^+ state of neutron-rich ^{16}C is studied in inverse kinematics using a 33-MeV/nucleon beam. The deformation parameter $\beta_{pp'} = 0.47(5)$ obtained is consistent with the global systematics of even-even nuclei, based on the homogeneous quantum liquid-drop model. This result contrasts that of a recent lifetime measurement for the 2_1^+ state in ^{16}C , where an anomalously reduced $E2$ transition strength is observed. A combination of these two results yields a large M_n/M_p ratio of about 7, indicating a dominant neutron contribution to the quadrupole collectivity.

DOI: [10.1103/PhysRevC.73.024610](https://doi.org/10.1103/PhysRevC.73.024610)

PACS number(s): 25.40.Ep, 23.20.Lv, 23.20.Js, 27.20.+n

I. INTRODUCTION

Research on unstable nuclei has achieved significant progress over the last few decades and several exotic features not encountered in normal stable nuclei have been reported. New forms of nuclear matter such as the neutron halo or skin [1] have been observed, and the dramatic evolution of nuclear shell structure have been revealed for nuclei with large isospin asymmetries. Anomalous features have also been noted in the dynamic behaviors of nuclei, manifested through the properties of nuclear excitations; for example, enormously strong soft dipole ($E1$) excitations [2] and reduced electric quadrupole ($E2$) polarization charges [3] have been reported in very neutron rich nuclei and have been related to decoupling effects of valence neutrons from the core nucleus. An anomalously small $E2$ transition strength recently observed in ^{16}C [4] may be evidence of unusual dynamics in which protons and neutrons exhibit very different behaviors.

The $E2$ transition strength is a fundamental nuclear quantity that reflects the static or dynamic deformation of a charged particle distribution in a nucleus. The reduced $E2$ transition probability $B(E2)$ from the first 2^+ (2_1^+) state to the ground 0^+ ($0_{g.s.}^+$) state for an even-even nucleus has long been used as a basic observable in extracting the magnitude of a nuclear quadrupole ($E2$) collectivity. A simple collective model treating a nucleus as a homogeneous quantum liquid-drop has been quite successful in describing the systematic tendency of $B(E2)$, predicting that $B(E2)$ varies in inverse proportion to the excitation energy $E(2_1^+)$ [5]. Contrary to this, the $B(E2)$ value obtained recently through a lifetime

measurement of the 2_1^+ state in ^{16}C was found to be remarkably small despite the small $E(2_1^+)$ value of 1.77 MeV [4]. This result indicates an unexpectedly small contribution of protons to the strength of the excitation to the 2_1^+ state. This finding raises an intriguing question as to whether or not the neutron contribution is similarly small for the relevant quadrupole excitation. A large difference between the proton and neutron contributions has been reported in a recent work on Coulomb-nuclear interference in $^{208}\text{Pb}+^{16}\text{C}$ inelastic scattering [6]. Definitive studies using other probes with enhanced sensitivity to neutrons should be necessary to answer this question.

The present article reports inelastic proton scattering (p, p') on ^{16}C observed at 33 MeV/nucleon, to determine the neutron collectivity of the 2_1^+ state. To deduce the magnitude of the neutron collectivity, we have combined the (p, p') data with the lifetime measurement [4]. While lifetime measurement only probes the proton (or charge) contribution to the quadrupole excitation, proton inelastic scattering is sensitive to both proton and neutron contributions. Thus a combination of these two measurements allows one to disentangle the proton and neutron collectivities for the 2_1^+ state.

A great advantage of using inelastic proton scattering lies in its sensitivity to neutrons. This is ascribed to the property of internucleon interactions in which the proton-neutron interaction is about three times stronger than the interactions between like nucleons (proton-proton or neutron-neutron) [7]. Due to this, the proton probe has a higher sensitivity to neutrons compared to the heavy-ion probes. For the study of low-energy collective excitations, inelastic proton scattering has further advantages. First, extensive and systematic study of proton elastic scattering has led to the development of a useful simple procedure for finding adequate sets of optical potential parameters. This procedure can be used for extracting reliable spectroscopic information from (p, p') data. Second, proton

*Electronic address: onghjin@nucl.phys.s.u-tokyo.ac.jp

†Present address: Physics Division, ANL, Argonne, IL, USA.

inelastic scattering is a well-established probe for determining the magnitude of quadrupole collectivity. A rich accumulation of data allows us to make a systematic comparison over a wide range of the nuclear chart, which has singled out the exotic behavior of ^{16}C , as shown later.

In the present experiment, we used the technique of in-beam γ -ray spectroscopy, incorporating inelastic proton scattering in inverse kinematics [8]. Unlike the missing mass method, this technique allows for the use of a thick target, which is a great advantage when investigating nuclei far from stability. The feasibility of this method is further enhanced by the use of a liquid hydrogen target [9].

II. EXPERIMENT

The experiment was performed at the RIKEN Accelerator Research Facility. A secondary beam of ^{16}C was obtained in a fragmentation reaction using a 94-MeV/nucleon ^{40}Ar primary beam with a typical intensity of 60 pA incident on a 740-mg/cm 2 ^9Be target. Fragments produced were isotope-separated in flight by the RIKEN Projectile Fragment Separator (RIPS) [10] to produce a ^{16}C beam at the exit. The intensity of the ^{16}C beam was about 6×10^3 counts per second. The energy of the incident ^{16}C was obtained by a time-of-flight (TOF) measurement using two 1-mm thick plastic scintillators (PLs) placed 518 cm apart along the beam line. Particle identification was performed by combining the TOF and ΔE information, measured with the PLs. The ^{16}C beam had a purity of around 24%, with ^{19}O and ^{20}F as contaminants. The incident beam bombarded a liquid hydrogen target with an effective thickness of 225 ± 8 mg/cm 2 . The energy of the ^{16}C beam was estimated to be 33 MeV/nucleon at the center of the target.

Scattered particles were detected with a counter telescope placed downstream of the target. The telescope consisted of a stack of Si detectors and a parallel plate avalanche counter (PPAC). The stack of Si detectors comprised four layers, each with four Si detectors of the same thickness arranged in a 2×2 matrix. The thicknesses of the four layers were 0.5 mm, 0.5 mm, 1.0 mm, and 0.5 mm. Each Si detector had an effective area of 50×50 mm 2 . Most of the scattered ^{16}C particles were stopped in the third layer of the telescope; the counters in the last layer served as veto counters to reject events due to light particles. The PPAC was used to obtain timing signals and was also used together with two upstream PPACs to measure the scattering angles of the ^{16}C particles. Identification of the scattered particles was performed using the standard TOF- ΔE and ΔE - E methods. The counter telescope covered angles up to 4.5° with respect to the beam axis. Note that the kinematic limit for the laboratory scattering angle of ^{16}C was 3.6° . The acceptance of the telescope was estimated using a Monte Carlo simulation that took into account the finite size and angular spread of the incident beam, multiple scattering in the target (about 0.7 degrees in rms), and the detector geometry including the gaps between the Si detectors. By further considering the angular distribution of (p , p') scattering on ^{16}C , the acceptance was found to effectively cover $73 \pm 5\%$ of the angle-integrated cross section of the inelastic scattering.

The deexcitation γ rays were detected by a NaI(Tl) array consisting of 105 scintillators, which form part of the DALI2

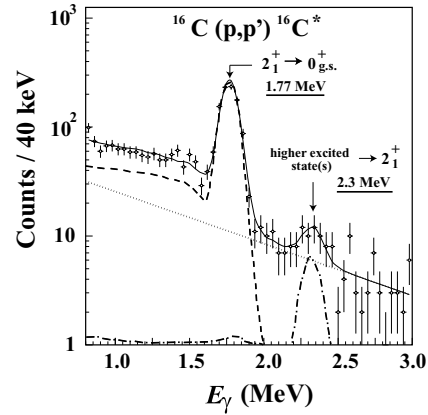


FIG. 1. Doppler-shift corrected γ -ray energy spectrum obtained in coincidence with scattered ^{16}C particles. The γ -ray yield was determined by fitting the energy spectrum with the solid curve, which was obtained by summing the GEANT-simulated energy spectra for the 1.77 MeV γ rays (dashed) and the γ rays from the higher excited states (dash-dotted), and an exponential function (dotted).

[11]. The NaI(Tl) array, arranged coaxially with respect to the beam axis, covered a polar angular range of 25 – 150° . The typical energy resolution was 3.0% in rms for 1275-keV γ rays as measured with a ^{22}Na standard source.

III. RESULTS

To determine the angle-integrated cross section, the yield of γ rays associated with the $2_1^+ \rightarrow 0_{g.s.}^+$ transition was first deduced. Figure 1 illustrates the Doppler-shift corrected energy spectrum of γ rays obtained in coincidence with inelastically scattered ^{16}C particles. A full-energy peak corresponding to the $2_1^+ \rightarrow 0_{g.s.}^+$ transition is clearly seen at 1.77 MeV. In addition, γ decays from higher excited states are observed at energies around 2.3 MeV. No other significant peaks are observed. To produce the energy spectrum, Monte Carlo simulations using the GEANT code [12] were carried out. The dashed and the dash-dotted curves shown in the figure represent the GEANT-simulated energy spectra for the 1.77 MeV and higher excited states while the dotted curve represents an exponential background. As shown in Fig. 1, the yield of γ rays was obtained by fitting the energy spectrum with the solid curve, which was obtained by summing the simulated curves and the background. The feeding contribution from the higher excited states, estimated to be $4 \pm 1\%$, was subtracted. The angle-integrated cross section was determined to be 22.6 ± 3.2 mb. Note that the uncertainty includes both statistical (3%) and systematic (14%) uncertainties. The systematic uncertainties are mainly attributed to the uncertainties in (i) the estimation of the detraction of the inelastic cross section due to break-up effect (9%), (ii) the determination of the Si acceptance (7%), (iii) the determination of the effective thickness of the liquid hydrogen target (4%), and (iv) the determination of the transmission of the ^{16}C beam at the target (4%).

The angle-integrated cross section thus obtained can be used to extract the nuclear deformation parameter $\beta_{pp'}$. For this purpose we incorporated distorted-wave Born approximation (DWBA) calculations using the ECIS79 code [13] in the

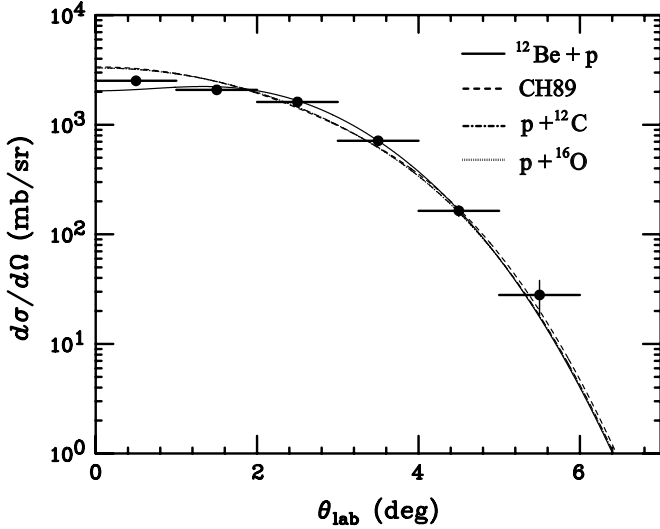


FIG. 2. Differential cross section for inelastic $0_{g.s.}^+ \rightarrow 2_1^+$ transition in ^{16}C . The dots with error bars, which are purely statistical, represent the experimental data. The four curves are the theoretical ones obtained through ECIS calculation. The solid, dashed, dash-dotted and dotted curves correspond to the optical potential obtained from $^{12}\text{Be}+p$, CH89, $p+^{12}\text{C}$ and $p+^{16}\text{O}$ elastic scattering.

framework of the vibrational model. In the calculation, $\beta_{pp'}$ represents the oscillator strength determining the cross section of the inelastic scattering. The subscript pp' is used to distinguish this parameter from different values of the nuclear deformation parameter, which may vary depending on the probing process.

Since the optical potential parameters are not known for the elastic proton scattering on ^{16}C , in our calculations, we have tested four optical potential parameters, namely the global phenomenological optical-model parameter set CH89 proposed in Ref. [14], optical potential parameters obtained from $p+^{16}\text{O}$ elastic scattering at 34 MeV, $p+^{12}\text{C}$ elastic scattering at 31 MeV [15] and $^{12}\text{Be}+p$ elastic scattering at 55 MeV [16].

For each potential parameter set, we adjusted the deformation parameter $\beta_{pp'}$ to reproduce the experimental angle-integrated cross section. The angular distribution of the differential cross sections was then compared with the experimental data. Figure 2 shows the angular distributions of the differential cross sections. The vertical error bars in the figure represent the statistical errors for the differential cross sections while the horizontal error bars represent the bin size. The angular resolution of the scattered particles was about 1.0° in rms in the present experiment. The solid, dashed, dash-dotted, and dotted curves represent the theoretical calculations obtained with optical-model potential from $^{12}\text{Be}+p$, CH89, $p+^{12}\text{C}$ and $p+^{16}\text{O}$, respectively. In reproducing the theoretical curves, we had considered the experimental angular resolution. Except for the data point in the forward angle near 0° , all of the four curves reproduced the experimental data equally well. Since no clear preference between the four was found, we adopted average values over the four sets of optical parameters. The $\beta_{pp'}$ values obtained are shown in Table I together with the deformation lengths ($\delta_{pp'} = \beta_{pp'} R = \beta_{pp'} r_0 A^{1/3}$). Taking the

TABLE I. Nuclear deformation parameter $\beta_{pp'}$ and deformation length $\delta_{pp'}$ deduced from DWBA calculations.

Optical potential	$\beta_{pp'}$	r_0 (fm)	$\delta_{pp'}$ (fm)
CH89 [14]	0.476(37)	1.16	1.39(11)
$p+^{16}\text{O}$ [15]	0.440(33)	1.14	1.26(9)
$p+^{12}\text{C}$ [15]	0.531(42)	1.10	1.47(12)
$^{12}\text{Be}+p$ [16]	0.435(32)	1.48	1.62(12)

standard deviation as an additional systematic error, $\beta_{pp'}$ and $\delta_{pp'}$ were determined to be 0.47 ± 0.05 and 1.44 ± 0.17 fm.

IV. DISCUSSION

In the homogeneous quantum liquid-drop model, protons and neutrons contribute equally to the quadrupole collectivity and the value of the deformation parameter is thought to be independent of the probing process, so that the deformation parameter for electromagnetic transitions β_{em} has the same value as $\beta_{pp'}$. A general reference for the magnitude of the deformation parameter can then be found in the following equation, which represents the systematic behavior of β_{em} [5]:

$$\beta_{sys} = (466 \pm 41) A^{-1} (E(2_1^+) (\text{keV}))^{-1/2}. \quad (1)$$

Here, the deformation parameter predicted systematically is denoted as β_{sys} to distinguish it from the experimental values. Note that the deformation parameter is simply given as a function of mass number A and excitation energy $E(2_1^+)$.

Figure 3(a) shows $\beta_{pp'}/\beta_{sys}$ ratios for even-even nuclei over a wide range of the nuclear chart. The ratio for ^{16}C deduced

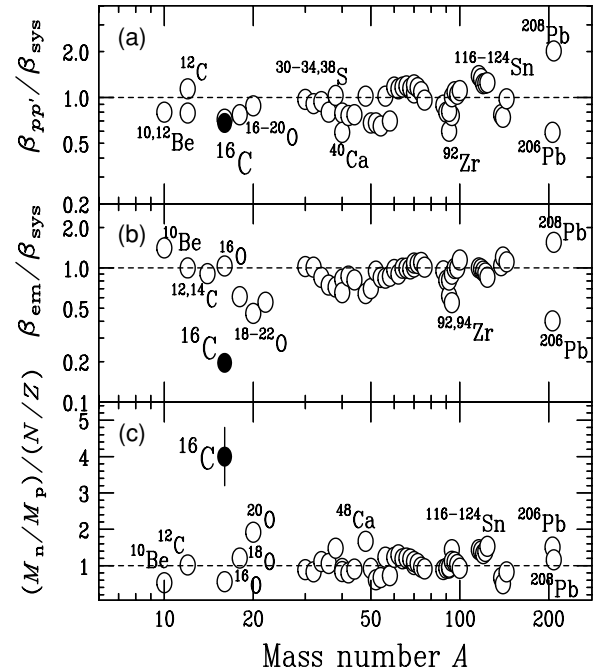


FIG. 3. Ratios of deformation parameters (a) $\beta_{pp'}/\beta_{sys}$, (b) β_{em}/β_{sys} , and (c) double ratio of proton and neutron quadrupole matrix elements $(M_n/M_p)/(N/Z)$ of the lowest 2^+ states of even-even nuclei. See text for details.

from the present $\beta_{pp'}$ results is shown as a filled circle. The $\beta_{pp'}$ data for the other nuclei are mostly obtained from the tabulation in Ref. [17]. Except for a few cases, such as the doubly closed shell ^{208}Pb , the ratios for even-even nuclei are confined in a fairly narrow domain of 65% to 135% of the predicted values. The ratio of 0.68 ± 0.09 obtained for ^{16}C is smaller than unity but falls within the above domain. For comparison, $\beta_{\text{em}}/\beta_{\text{sys}}$ ratios are also presented in Fig. 3(b), with most of the data taken from Ref. [5]. In deriving the ratio we noted that β_{em} is proportional to $Z/\sqrt{B(E2)}$. It is clearly seen that the $\beta_{\text{em}}/\beta_{\text{sys}}$ ratio of 0.20 for ^{16}C [4] is considerably smaller than those for any other nuclei, including closed shell nuclei. The sharp contrast between the moderate-sized $\beta_{pp'}/\beta_{\text{sys}}$ and the extremely small $\beta_{\text{em}}/\beta_{\text{sys}}$ indicates that the proton and neutron contributions are quite different in promoting quadrupole collectivity of the 2_1^+ state in ^{16}C .

A more quantitative analysis of the relative importance of proton and neutron contributions can be made by introducing the neutron and proton transition matrix elements M_n and M_p as defined in Ref. [7]. One can separately determine M_n and M_p from $\delta_{pp'}$ and δ_{em} by using their different sensitivities to the proton and neutron contributions. According to Bernstein the double ratio $(M_n/M_p)/(N/Z)$ can be obtained through the following equation [7]:

$$\frac{M_n}{M_p} = \frac{b_p}{b_n} \left[\frac{\delta_{pp'}}{\delta_{\text{em}}} \left(1 + \frac{b_n}{b_p} \frac{N}{Z} \right) - 1 \right]. \quad (2)$$

For (p, p') at intermediate energies, the ratio of the interaction strengths of scattered protons with neutrons and with protons b_n/b_p is about 3 [7]. From the lifetime measurement, the magnitude of δ_{em} is deduced to be 0.41 ± 0.06 fm [4]. Combining with the present $\delta_{pp'}$ result one obtains $|(M_n/M_p)/(N/Z)| = 4.0 \pm 0.8$, and $|M_n/M_p| = 6.7 \pm 1.3$, assuming the same sign for the two deformation parameters. This result is consistent with the M_n/M_p ratio of 7.6 ± 1.7 reported in Ref. [6].

To depict the significance of the present result, in Fig. 3(c) we compare the double ratio $(M_n/M_p)/(N/Z)$ deduced for even-even nuclei over a wide range of the nuclear chart. We find that the value for ^{16}C is much greater than the standard value of unity [dashed-line in Fig. 3(c)] expected for a homogeneous quantum liquid-drop, and is by far the largest value within the data available; it is greater by a factor of nearly two than the values for ^{48}Ca [18] and ^{20}O [19], which were considered to represent rare cases of exceptionally large $(M_n/M_p)/(N/Z)$.

The anomalously large $(M_n/M_p)/(N/Z)$ observed for ^{16}C indicates a predominant contribution of neutrons to the quadrupole collectivity of the 2_1^+ state. The comparison between Figs. 3(a) and 3(b) further reveals that the relative importance of neutrons primarily arises from the extremely quenched proton collectivity rather than from the magnitude of the neutron collectivity, which is found to be only moderate.

According to a shell-model calculation, the quenched proton contribution is related to the formation of a hard proton closed shell and a soft neutron open shell in ^{16}C [20]. In this model, almost all contributions to $B(E2; 2_1^+ \rightarrow 0_{\text{g.s.}}^+)$ arise from valence neutrons, as protons are barely excited due to the increased magicity at $Z = 6$. The anomalously small $B(E2)$ of $0.63 e^2 \text{fm}^4$ [4] observed for ^{16}C may then require a significant reduction of the neutron effective charges [20]. In fact, Ref. [20] obtained a fairly small value of $B(E2) = 2.35 e^2 \text{fm}^4$ by using reduced effective charges, as discussed in Ref. [21].

A theoretical calculation was also made using antisymmetrized molecular dynamics (AMD) [22]. It has been suggested that the transition to the 2_1^+ state is mainly governed by a neutron deformation with a prolate shape, whose orientation primarily determines the principal axis of the total system. On the other hand, the contribution from protons, which tends to promote oblate deformation, is considerably reduced due to the deviation of the symmetric axis preferred by protons from that of the total system. This unusual structure of ^{16}C results in a $B(E2)$ value as small as $1.4 e^2 \text{fm}^4$. Both these theories indicate neutron dominance of the collectivity of the 2_1^+ state, while they give very small values of $B(E2)$. However, the theories tend to underestimate the quenching effect experimentally observed for $B(E2)$.

V. SUMMARY

In summary, we have observed inelastic proton scattering on ^{16}C at 33 MeV/nucleon in inverse kinematics. From the angle-integrated cross section for the $0_{\text{g.s.}}^+ \rightarrow 2_1^+$ transition, the deformation parameter and deformation length were determined to be 0.47 ± 0.05 and 1.44 ± 0.17 fm. In contrast to the case of δ_{em} , which was found to be anomalously small [4], the size of $\delta_{pp'}$ was found not to be quenched but to be typical. Thus the ratio of the neutron and proton quadrupole matrix elements $(M_n/M_p)/(N/Z)$ has an enormous magnitude of 4.0 ± 0.8 . Systematic experimental studies on neighboring nuclei as well as theoretical attempts to unify the different approaches would be helpful in further exploring the underlying mechanism of the anomalous quadrupole collectivity.

ACKNOWLEDGMENTS

We thank the RIKEN Ring Cyclotron staff members for providing a stable ^{40}Ar beam throughout the experiment. HJO is grateful to the Ministry of Education, Culture, Sports, Science and Technology of Japan (Monbukagakusho), and the Japan Society for the Promotion of Science for scholarships. This work was supported in part by a Grant-in-Aid for Scientific Research No. 15204017, No. 16740158 from Monbukagakusho, and OTKA T42733, T46901 (Hungary).

[1] I. Tanihata, H. Hamagaki, O. Hashimoto, Y. Shida, N. Yoshikawa, K. Sugimoto, O. Yamakawa, T. Kobayashi, and N. Takahashi, Phys. Rev. Lett. **55**, 2676 (1985); Phys. Lett. **B289**, 261 (1992).

[2] T. Nakamura *et al.*, Phys. Lett. **B394**, 11 (1997).

[3] H. Ogawa *et al.*, Phys. Lett. **B451**, 11 (1999).

[4] N. Imai *et al.*, Phys. Rev. Lett. **92**, 062501 (2004).

[5] S. Raman *et al.*, At. Data Nucl. Data Tables **78**, 1 (2001).

[6] Z. Elekes *et al.*, Phys. Lett. **B586**, 34 (2004).

- [7] A. M. Bernstein *et al.*, Comments Nucl. Part. Phys. **11**, 203 (1983).
- [8] H. Iwasaki *et al.*, Phys. Lett. **B481**, 7 (2000).
- [9] Y. Yanagisawa *et al.*, Phys. Lett. **B566**, 84 (2003).
- [10] T. Kubo *et al.*, Nucl. Instrum. Methods B **70**, 309 (1992).
- [11] S. Takeuchi *et al.*, RIKEN Accel. Prog. Rep. **36**, 148 (2003).
- [12] GEANT3: Detector Description and Simulation Tool, CERN program library.
- [13] J. Raynal, NOTES ON ECIS79, unpublished.
- [14] R. L. Varner *et al.*, Phys. Rep. **201**, 57 (1991).
- [15] C. M. Perey and F. G. Perey, At. Data Nucl. Data Tables **17**, 1 (1976).
- [16] A. A. Korshennikov *et al.*, Phys. Lett. **B343**, 53 (1995).
- [17] M. A. Kennedy, Phys. Rev. C **46**, 1811 (1992); E. Fabrici, S. Micheletti, M. Pignanelli, F. G. Resmini, R. DeLeo, G. D'Erasmus, and A. Pantaleo, *ibid.* **21**, 844 (1980).
- [18] A. E. Feldman *et al.*, Phys. Rev. C **49**, 2068 (1994).
- [19] J. K. Jewell *et al.*, Phys. Lett. **B454**, 181 (1999); E. Khan *et al.*, *ibid.* **B490**, 45 (2000).
- [20] R. Fujimoto, Ph.D. thesis, University of Tokyo, 2003; T. Otsuka *et al.* (private communication).
- [21] H. Sagawa and K. Asahi, Phys. Rev. C **63**, 064310 (2001).
- [22] Y. Kanada-En'yo and H. Horiuchi, Phys. Rev. C **55**, 2860 (1997); Y. Kanada-En'yo, *ibid.* **71**, 014310 (2005).